Experimental observation of initial-state effects in photo-double-ionization of Ne 2*s*

P. Bolognesi,[1] R. Flammini,[1] A. Kheifets,[2] I. Bray,[3] and L. Avaldi[1,4]
[1]*CNR–Istituto di Metodologie Inorganiche e dei Plasmi, Area della Ricerca di Roma 1, CP 10, 00016 Monterotondo Scalo, Italy*
[2]*Research School of Physical Sciences and Engineering, Australian National University, Canberra, Australia*
[3]*School of Engineering Science, Murdoch University, Perth, Western Australia*
[4]*INFM-TASC, Gas Phase Photoemission Beamline at Elettra, Area Science Park, Trieste, Italy*
(Received 14 May 2004; published 20 December 2004)

The triple-differential cross section (TDCS) for the photo-double-ionization of Ne and He leading to the $Ne^{2+}(2s^{-2}2p^6)$ and $He^{2+}(1s^{-2})$ states have been measured 20 eV above their respective thresholds in equal energy sharing conditions. The experimental results show that the Ne TDCS's are qualitatively different from the He ones. A calculation using the convergent close coupling method with a He-like final state and different initial-state wave functions clearly shows that the observed differences can be ascribed to an initial-state effect.

DOI: 10.1103/PhysRevA.70.062715 PACS number(s): 32.80.Fb

I. INTRODUCTION

During the past decade, a great experimental and theoretical effort [1–3] has been devoted to studying the photo-double-ionization (PDI) of He. This is because this process provides unique information on electron correlation. Indeed the ejection of two electrons by the absorption of a single photon only occurs via electron correlation. He is the archetypal system to study PDI because the final doubly charged ion state has the simplest $^1S^e$ symmetry and therefore the final state of the electron pair is of a pure $^1P^o$ symmetry. Moreover, the He double-ionization continuum is free of resonant processes. The complete experimental characterization of PDI implies experiments in which either the two photoelectrons [4] or one of the photoelectrons and the residual ion [5] are detected in coincidence. In such experiments the triple-differential cross section $d^3\sigma/d\Omega_1 d\Omega_2 dE_1$ (TDCS)—i.e., a cross section which is differential in the angles of emission of the two photoelectrons $\Omega_1=(\vartheta_1,\varphi_1)$ and $\Omega_2=(\vartheta_2,\varphi_2)$ and in one kinetic energy E_1—is measured. The kinetic energy E_2 of the other electron is determined by energy conservation—i.e., $E_2=h\nu-I^{2+}-E_1$, where I^{2+} is the double-ionization potential. Since the first experimental determination of the He TDCS in 1993 [4] a large set of data from the near-threshold [6] region up to a photon energy of about 450 eV [7] has been published. The main characteristics of the process appear to be determined by the correlated motion of the two ejected electrons in the field of the doubly charged ion. Indeed Maulbetsch and Briggs [8] performed detailed calculations of the He TDCS with an initial state represented either by a simple product of hydrogenic uncorrelated wave functions or by a Hylleraas correlated wave function. They have shown that the shapes of the resulting TDCS are practically indistinguishable provided that an accurate three-body final-state wave function is used. Similar results have been found in the framework of the hyperspherical *R*-matrix method with semiclassical outgoing waves (HRM-SOW) by Malegat *et al.* [9]. Conversely, the absolute value of the TDCS depends on the used initial wave function, because the overall probability of PDI strongly depends on small radial distance correlations.

The effects of the initial-state orbital on the shape of the TDCS were investigated experimentally in the case of Ne^{2+} ($2p^{-2}\ ^3P^e$, $^1D^e$, and $^1S^e$) [10–12] and $Xe^{2+}(5p^{-2}\ ^1S^e)$ [13]. The case of the $Ne^{2+}\ ^1S^e$ state is of particular interest in this work because it can be directly compared with He. The experimental data of the Freiburg and Paris groups [10–12] on Ne display a shape of the TDCS with two extra lobes at a relative angle $\vartheta_{12}\leqslant 90°$ and a narrowing of the main lobes with respect to the He TDCS measured at the same excess energy and in the same kinematics. A simple model based on the initial uncorrelated $2p^2\ ^1S^e$ state, which restricts the possible continuum final states to only two (the $\varepsilon s\varepsilon p$ and $\varepsilon p\varepsilon d$ ones), and a proper correlation factor, which accounts for the interaction of the two free electrons, allowed those authors to reproduce satisfactorily the measured TDCS and to interpret the new features as due to the interference of the two channels. A further theoretical work by Malcherek *et al.* [14] who again used as initial state a simple p^2 product wave function evaluated in the Hatree-Fock potential of the neutral atom and a final state of the 3-Coulomb form used for He, confirmed this interpretation, although the experimental minima between the two lobes are much deeper than the theory predicts. The experiment near threshold in Xe [13] produced a shape of the TDCS with more structures than the He one and the analysis showed a correlation width narrower that the one measured in He. Kazansky and Ostrovsky [15] have shown that the relative intensity of the secondary structure in Xe is quite sensitive to the degree of initial-state correlation. On the other hand, the same model predicted TDCS in reasonable agreement with the Ne data discussed above [10–12] employing uncorrelated initial-state wave functions [16].

About 25 years ago Neudatchin *et al.* [17] proposed photo-double-ionization as a tool to obtain information on electron correlation in the target initial state and therefore to discriminate between different bound-state wave functions, which account in different ways for electron correlation. More recently some calculations in the framework of the extended Wannier ridge model [18] have predicted that the difference in the radial density distributions of the initial one-electron *ns* orbitals of the alkaline-earth-metal atoms with respect to the He one should produce qualitative differ-

ences in the measured TDCS. Fully numerical calculations of the Be^{2+} $(2s^{-2})$ TDCS supported this claim [19,20]. In the present work we have investigated the possibility to use the shape of the TDCS to probe the quality of the initial-state wave functions. To this purpose we have measured the photo-double-ionization of Ne and He leading to the $Ne^{2+}(2s^{-2}2p^6)$ and $He^{2+}(1s^{-2})$ states at about 20 eV above their respective thresholds in equal energy sharing conditions. The symmetries of both the residual ion and electron pair in the final state, $^1S^e$ and $^1P^o$, respectively, as well as the kinetic energy of the ejected electrons are the same. The double-ionization potential of the $Ne^{2+}(2s^{-2}2p^6)$ state, 121.9 eV [21–23], is lower than the binding energy of the ^4S ground state of the Ne^{3+} ion [23]. Thus decay to the triple continuum is not allowed. Moreover, the measurements of the $Ne^{2+}(2s^{-2}2p^6)$ partial ionization cross section using photon-induced fluorescence spectroscopy [22] did not provide evidence of resonances at 142 eV, the incident energy of the present measurements, which may lead to photo-double-ionization via an indirect process. Therefore the present experiment probes the direct photo-double-ionization of both He $1s^2$ and Ne $2s^2$ shells.

II. EXPERIMENT

The experiments have been performed at the Gas Phase Photoemission beamline [24] of the Elettra storage ring using the multicoincidence end station [25]. Two independently rotatable turntables are housed in the vacuum chamber. Seven hemispherical electrostatic spectrometers are mounted at 30° angular intervals on a turntable that rotates in the plane perpendicular to the direction, **z**, of propagation of the incident radiation, while three other spectrometers are mounted at 0°, 30°, and 60° with respect to the polarization vector ε of the light on a smaller turntable. In these measurements both the arrays have been kept in the perpendicular plane. The energy resolution and the angular acceptance in the dispersion plane of the spectrometers in these measurements were $\Delta E = 0.120$ eV and $\Delta\vartheta = \pm 3°$, respectively. The main part of the coincidence electronics is made by three independent time-to-digital converters (TDC's). In the experiment each TDC unit is operated in the common start mode with the signals of each one of the three analyzers of the small turntable used as starts and the signals from the other seven as stops. In this way 21 coincidence pairs are collected simultaneously. The angular distribution is obtained by successive rotations of the larger frame. The relative efficiency of the spectrometers has been calibrated via the measurement of the photoelectron angular distribution of $He^+(n=3)$ at 10 eV above its threshold. At this energy the β value is known [26]. Then the obtained efficiencies have been confirmed by determining the β of the photoelectron angular distribution of $He^+(1s^{-1})$ at the same kinetic energy. The same efficiency correction has been assumed for the coincidence measurements. The validity of this assumption has been tested by measuring the coincidence yield at two positions of the larger turntable, which allows to overlap two nearby analyzers. Therefore all the experimental data are internormalized and can be reported on a common scale of counts.

III. RESULTS AND DISCUSSION

The experimental TDCS's for the $Ne^{2+}(2s^{-2}2p^6)$ state are reported in Fig. 1. The TDCS's of He at an excess energy $E = 20$ eV and equal energy sharing have been measured by several groups and calculated by all the most recent theories [3,27]. General agreement has been achieved among the different experiments as well as between experiments and theories. The present results are in good agreement with all previous data. Therefore for the sake of clarity instead of showing the He results in a separate figure we have reported their best representation as the solid curve in Fig. 1. This has been obtained in the following way. By considering the invariance with respect to rotation around the electric vector direction of the incident radiation and the general properties of the spherical harmonics the geometrical factors and the dynamical parameters of the TDCS can be separated. This leads to a parametrization of the TDCS [28], which in the case of an incident radiation that propagates along the **z** axis and is fully linearly polarised along the $\boldsymbol{\varepsilon} = \varepsilon \mathbf{x}$ axis can be written as

$$d^3\sigma/d\Omega_1 d\Omega_2 dE_1 \propto |a_g(E_1,E_2,\vartheta_{12})(\cos\vartheta_1 + \cos\vartheta_2) + a_u(E_1,E_2,\vartheta_{12})(\cos\vartheta_1 - \cos\vartheta_2)|^2, \quad (1)$$

where ϑ_1 and ϑ_2 are the angles of emission of the two photoelectrons with respect to ε and ϑ_{12} is the relative angle between the two. The complex amplitudes a_g and a_u are respectively symmetric and antisymmetric relative to the exchange of E_1 and E_2. The ϑ_{12} and energy dependence of these amplitudes include all the physical information on the dynamics of the process—i.e., the effects of the electron-electron and electron-residual ion interactions. In the case of equal energy sharing, $a_u = 0$, and thus the TDCS reduces to a simple form. Since the first measurements of the TDCS, the square modulus $|a_g|^2$ of the symmetric amplitude, often called in the literature the "correlation factor," has been represented by a Gaussian function

$$|a_g|^2 \propto \exp[-4\ ln\ 2(\vartheta_{12} - 180)^2/\vartheta_{1/2}{}^2], \quad (2)$$

where $\vartheta_{1/2}$ is the correlation width. This form follows from the Wannier-type theories [29,30] in which the angular variation near the Wannier saddle decouples from the radial motion [31] and can be described by the ground-state wave function of an harmonic oscillator. These models are expected to be valid only at small excess energies. However, it turned out that the Gaussian form may be used as a useful approximation to describe several He experiments at higher excess energy [27]. More recently Kheifets and Bray [32] supported the validity of the Gaussian parametrization for He via a fully numerical calculation in the range of excess energy 3–80 eV. Thus the solid curve in Fig. 1 is a representation of the experimental He TDCS using Eqs. (1) and (2) with a correlation width $\vartheta_{1/2} = 91°$. The comparison of the He and Ne results clearly shows that in both targets the number

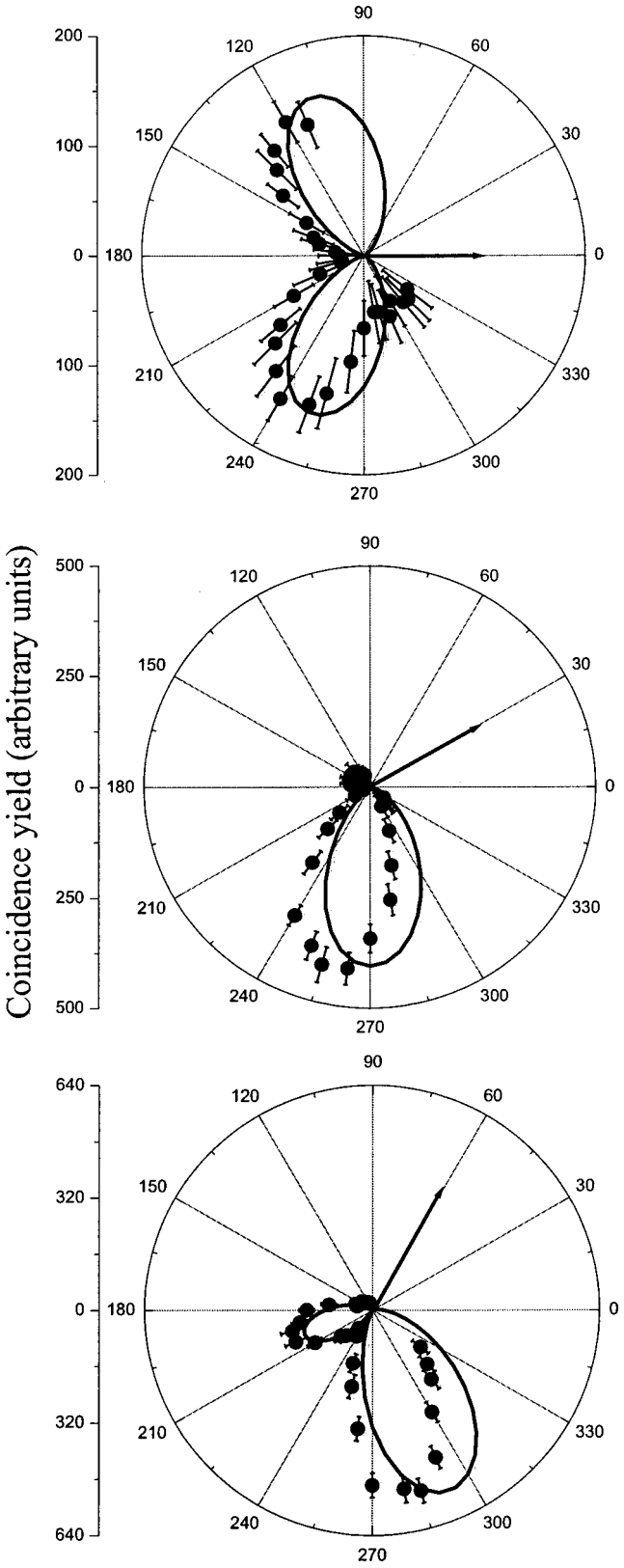

FIG. 1. The TDCS of the $Ne^{2+}(2s^{-2})$ measured at 20 eV excess energy in equal energy sharing conditions, perpendicular geometry, and three different directions of ejection of the fixed electron—i.e., 0°, 30°, and 60° (dots) with respect to the polarization axis of the photon beam. The solid line is the representation (see text) of the TDCS of He^{2+} measured in the same kinematics.

and relative intensity of the lobes of the TDCS are the same, but for a small feature at $280° \leqslant \vartheta_2 \leqslant 330°$ in the Ne TDCS measured at $\vartheta_1 = 0°$. However, the position and width of the lobes are quite different. In particular the lobes of the Ne TDCS are narrower than the ones in He. The present findings cannot be attributed to the different I^{2+}/E ratio, this being $1/4$ and $1/6$ for the He and Ne cases, respectively. Indeed the He TDCS for an excess energy of 13 eV—i.e., for the same I^{2+}/E ratio as for the Ne case—can be calculated with Eqs. (1) and (2) using $\vartheta_{1/2} = 82°$ [6]. This results in a narrowing of the lobes of $\leqslant 10\%$ and in a shift of their position towards smaller ϑ_2 of about 5°.

The narrowing of the lobes in conjunction with the small feature observed at $\vartheta_1 = 0°$ is a clear indication of stronger angular correlations in Ne. Considering that in both cases the two electrons are ejected from an s^2 shell, they have the same kinetic energies in the continuum and the electron pairs in the final state have the same $^1P^o$ symmetry; then, the observed differences have to be ascribed to the different structure of the targets. Moreover, the small feature in the region $\vartheta_{12} \leqslant 90°$ resembles the one observed in the TDCS of the $Ne^{2+}(2p^{-2}{}^1S^e)$ [10–12]. In that case the symmetry of the doubly charged ion and of the electron pair were the same of He, but two p electrons were involved. Thus the feature was attribute to the p character of the initial state.

The difference observed in the $He^{2+}(1s^{-2})$ and $Ne^{2+}(2s^{-2})$ TDCS's may be due either to the different initial state or to a different interaction of the two ejected electrons with the residual ion. To isolate the contribution of the initial-state effects we have performed a calculation using the convergent close coupling (CCC) method [33]. This method is a fully numerical approach and relies on intensive computation. For the final state it solves the Schrödinger equation for the system of a photoelectron scattering on a singly charged ion by employing the close coupling expansion of the total wave function. The PDI results from the electron impact ionization of the ion. The He CCC integrated PDI cross sections and TDCS agree with the experimental ones over a broad energy range [34]. The CCC predictions are compared with the present He data in the top part of Fig. 2. In order to have a more compact view, we compare the square modulus of the experimental amplitude, $|a_g|^2$, obtained by the raw data divided by the kinematical factor of formula (1), with the calculated ones. Where multiple experimental determinations exist, a weighted average was calculated and plotted in Fig. 2. The theoretical calculations were rescaled to the experiment at $\vartheta_{12} = 150°$. In the inset of the figure the TDCS measured for $\vartheta_1 = 30°$ is also reported. Good agreement is observed between theory and experiment in both the $|a_g|^2$ and the TDCS.

In order to calculate the $Ne^{2+}(2s^{-2}2p^6)$ TDCS a He-like final state has been adopted in which the two photoelectrons depart in the field of the positive charge $Z=2$. As to the initial state, different Ne $2s$ wave functions were used. The simplest noncorrelated ground state was obtained by performing a self consistent Hartree-Fock calculation using the computer code by Chernysheva *et al.* [35]. It is well known that the intershell many-electron correlation affects significantly the ns-shell photoionization of the noble gas atoms [36]. In the case of Ne, the incident photon polarizes strongly

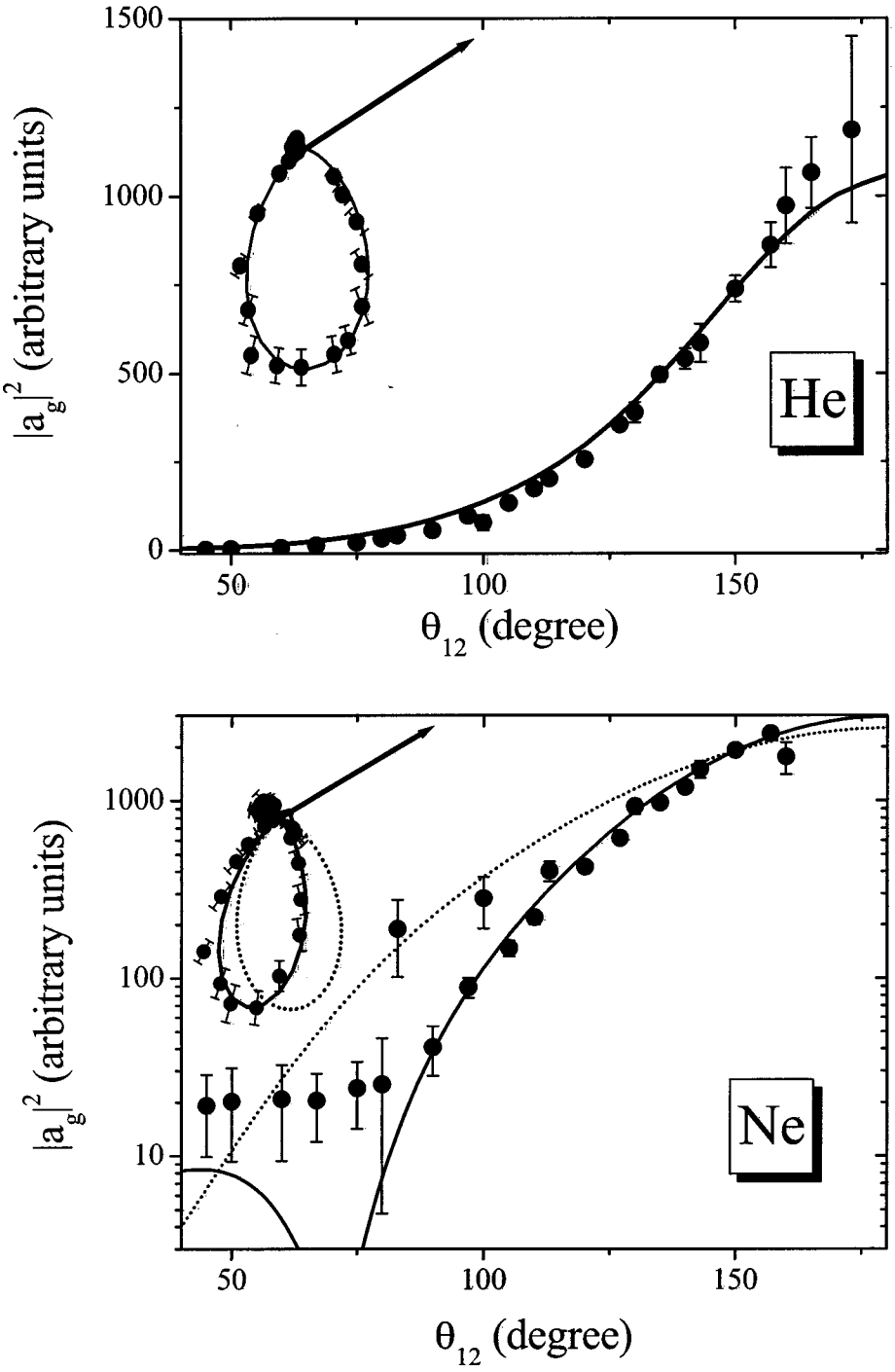

FIG. 2. The square modulus of the amplitude, $|a_g|^2$, obtained from the experimental TDCS of He^{2+} (top panel) and $Ne^{2+}(2s^{-2})$ (bottom panel) at $E=20$ eV and equal energy sharing versus the relative angle θ_{12}. The experimental results are compared with the predictions of the CCC model. In the bottom panel the calculations with the noncorrelated ground state $2s^2$ (dashed line) and the mixed ground state $C_{2s}2s^2+C_{2p}2p^2$ (solid line) which accounts for intershell correlation are shown. In the insets the theoretical TDCS is compared with the experiment for $\vartheta_1=30°$.

the outer $2p^6$ subshell which subsequently relaxes and ionizes the inner $2s^2$ subshell. The CCC model can only account for two active electrons. The best possible way to incorporate the intershell correlations into the model is to create a composite, multiconfiguration ground state $C_{2s}2s^2+C_{2p}2p^2$ built on the basis of the Hartree-Fock orbitals. The configuration interaction coefficients C_{2s} and C_{2p} cannot be obtained from first principles. Rather, we treated them as adjustable parameters to obtain the best agreement with the experimental TDCS. The obtained coefficients $|C_{2s}|^2 \approx 0.8$ and $|C_{2p}|^2 \approx 0.2$ seem to be realistic when compared with another indicator of the strength of the intershell correlation: the spectroscopic factor of the $2s^2$ shell in Ne. Experimental values of the spectroscopic factor are 0.91 in photoionization [37] and 0.85 in electron impact ionization [38]. A similar amount of the $2s/2p$ mixing is required to reproduce correctly the $2s$ ionization potential [39].

The comparison of the CCC calculations employing different ground-state wave functions with the Ne results is shown in the bottom part of Fig. 2. Here the logarithmic scale has been adopted in order to outline the non-Gaussian behavior at small ϑ_{12}. The dashed line corresponds to the noncorrelated ground state $2s^2$ and the solid line represents the mixed ground state $C_{2s}2s^2+C_{2p}2p^2$ which accounts for intershell correlation. The inclusion of the correlation in the ground state decreases significantly the correlation width

$\vartheta_{1/2}$ of $|a_g|^2$, from 91° to 74°, and brings it in a much better agreement with the experiment. This is also proved by the TDCS at $\vartheta_1 = 30°$ shown in the inset of the figure.

IV. CONCLUSIONS

In conclusion we have measured and compared the TDCS's of the He $1s^2$ and Ne $2s^2$ shells at the same excess energy above the threshold in the equal energy sharing conditions. The shape of the Ne TDCS displays differences with respect to the He ones. It has been shown that these differences can be explained by the intershell ground-state correlation in Ne as supported by CCC calculations with He-like final state and two different Ne ground states. An admixture of about 20% of the $2p^2$ character to the noncorrelated Ne $2s^2$ ground state allows us to reproduce the shape of the experimental TDCS. This strength of the intershell mixing seems to be compatible with the values of the spectroscopic factor of the Ne $2s^2$ shell known from single-ionization experiments as well as configuration-interaction calculations of the $2s$ ionization potential. The importance of configuration mixing in Ne to calculate, for example, the intensities of Auger transitions was pointed out already in the 1960's [40], but this is the first time that trace of this effect is observed in the shape of the TDCS. Thus our results provide evidence that (i) the ground-state correlation can influence the shape of the TDCS of the PDI and therefore (ii) the TDCS can be used to discriminate among different initial-state wave functions. However, it is also unquestionable that a complete description of the observed TDCS implies an extension of the used model with a proper description of the correlation between the emitted electrons and the bound ones in the final state.

It would be interesting to apply the same theoretical approach used in this work to the analysis of the direct PDI of Ca^{2+} $(4s^{-2})$ at about 25 eV above threshold reported by Beyer *et al.* [41]. In that work a narrowing of the angular distribution as compared to the He one at the same excess energy has been observed. An application of the HRM-SOW method [42], restricted to the Wannier ridge, has shown that the stronger electron correlations in alkaline-earth-metal atoms result in a narrowing of the angular distribution and that the TDCS becomes very sensitive to the quality of the initial-state wave functions when approaching the threshold.

The findings of this work together with the results of recent $(e,3e)$ experiments on Ar [43] prove that double ionization is one among the most suited processes to study electron correlation in bound states.

[1] J. S. Briggs and V. Schmidt, J. Phys. B **33**, R1 (2000).
[2] G. C. King and L. Avaldi, J. Phys. B **33**, R215 (2000).
[3] P. Bolognesi, G. C. King, and L. Avaldi, Radiat. Phys. Chem. **70**, 207 (2003).
[4] O. Schwarzkopf, B. Krässig, J. Elminger, and V. Schmidt, Phys. Rev. Lett. **70**, 3008 (1993).
[5] J. Ullrich, R. Moshammer, R. Dörner, O. Jagutzki, V. Mergel, H. Schmidt-Böcking, and L. Spielberg, J. Phys. B **30**, 2917 (1997).
[6] A. Huetz and J. Mazeau, Phys. Rev. Lett. **85**, 530 (2000).
[7] A. Knapp *et al.*, Phys. Rev. Lett. **89**, 033004 (2002).
[8] F. Maulbetsch and J. S. Briggs, J. Phys. B **26**, 1679 (1993).
[9] L. Malegat, P. Selles, and A. Kazansky, Phys. Rev. A **60**, 3667 (1999).
[10] S. J. Schaphorst, B. Krässig, O. Schwarzkopf, N. Scherer, and V. Schmidt, J. Phys. B **28**, L233 (1995).
[11] S. J. Schaphorst *et al.*, J. Electron Spectrosc. Relat. Phenom. **76**, 229 (1995).
[12] B. Krässig, S. J. Schaphorst, O. Schwarzkopf, N. Scherer, and V. Schmidt, J. Phys. B **29**, 4255 (1996).
[13] D. Waymel, L. Andric, J. Mazeau, P. Selles, and A. Huetz, J. Phys. B **26**, L123 (1993).
[14] A. W. Malcherek, F. Maulbetsch, and J. S. Briggs, J. Phys. B **29**, 4127 (1996).
[15] A. K. Kazansky and V. N. Ostrovsky, J. Phys. B **28**, 1453 (1995).
[16] A. K. Kazansky and V. N. Ostrovsky, Phys. Rev. A **52**, 1775 (1995).
[17] V. G. Neudatchin, Yu. F. Smirnov, A. V. Pavlitchenkov, and V. C. Levin, Phys. Lett. **64A**, 31 (1977).
[18] A. K. Kazansky and V. N. Ostrovsky, J. Phys. B **30**, L835 (1997).
[19] A. S. Kheifets and I. Bray, Phys. Rev. A **65**, 012710 (2002).
[20] F. Citrini, L. Malegat, P. Selles, and A. K. Kazansky, Phys. Rev. A **67**, 042709 (2003).
[21] L. Avaldi *et al.*, J. Phys. B **30**, 5197 (1997).
[22] K. H. Schartner *et al.*, J. Phys. B **26**, L450 (1993).
[23] W. Persson *et al.*, Phys. Rev. A **43**, 4791 (1991).
[24] B. Diviacco *et al.*, Rev. Sci. Instrum. **63**, 388 (1992); P. Melpignano *et al.*, *ibid.* **66**, 2125 (1995).
[25] R. R. Blyth *et al.*, J. Electron Spectrosc. Relat. Phenom. **101–103**, 959 (1999).
[26] R. Wehlitz, B. Langer, N. Berrah, S. B. Whitfield, J. Viefhaus, and U. Becker, J. Phys. B **26**, L783 (1993).
[27] G. Turri *et al.*, Phys. Rev. A **65**, 034702 (2002).
[28] A. Huetz, P. Selles, D. Waymel, and J. Mazeau, J. Phys. B **24**, 1917 (1991).
[29] A. R. P. Rau, J. Phys. B **9**, L283 (1976).
[30] J. M. Feagin, J. Phys. B **17**, 2433 (1984).
[31] J. M. Rost, J. Phys. B **27**, 5923 (1994).
[32] A. S. Kheifets and I. Bray, Phys. Rev. A **65**, 022708 (2002).
[33] A. Kheifets and I. Bray, J. Phys. B **31**, L447 (1998); Phys. Rev. Lett. **81**, 4588 (1998).
[34] A. Kheifets and I. Bray, Phys. Rev. A **58**, 4501 (1998).
[35] L. V. Chernysheva *et al.*, Comput. Phys. Commun. **18**, 87 (1979).
[36] M. Ya. Amusia, *Atomic Photoeffect* (Plenum Press, New York, 1990).
[37] O. Samardzic, S. W. Braidwood, E. Weigold, and M. Brunger, Phys. Rev. A **48**, 4390 (1993).
[38] S. Svensson, B. Eriksson, N. Mårtensson, G. Wendin, and U. Gelius, J. Electron Spectrosc. Relat. Phenom. **47**, 327 (1988).

[39] A. S. Kheifets, J. Phys. B **28**, 3791 (1995).
[40] W. N. Asaad, Nucl. Phys. **66**, 494 (1965).
[41] H-J Beyer, J. B. West, K. J. Ross, and A. De Fanis, J. Phys. B **33**, L767 (2000).
[42] L. Malegat, F. Citrini, P. Selles, and P. Archirel, J. Phys. B **33**, 2409 (2000).
[43] A. Lahmam-Bennani, C. C. Jia, A. Duguet, and L. Avaldi, J. Phys. B **35**, L215 (2002).